JOURNAL OF AIRCRAFT
Vol. 45, No. 2, March–April 2008

Thermally Induced Loads of Fastened Hybrid Composite/Aluminum Structures

Chihdar Yang,* Wenjun Sun,† Waruna Seneviratne,‡ and Ananthram K. Shashidhar§
Wichita State University,
Wichita, Kansas 67260-0044

DOI: 10.2514/1.31776

Large composite structures have been increasingly used in the aviation industry. New applications of composite materials include primary structures such as aircraft fuselages. These large composite parts are sometimes attached, either by the fasteners or adhesive bonding, to metallic structures. Because of the large coefficient of thermal expansion mismatch between the metallic and composite structures, the temperature change from the aircraft assembly line to the actual flight condition induces high thermal stresses during flight in both the composite fuselage and aluminum frames. An experimental program was executed to determine the interaction between the fastened Z-shaped aluminum beams and the solid composite laminate. An analytical model was also developed to simulate the thermal/mechanical behavior of the hybrid composite/metal structure. Finite element analysis was conducted to determine the parameters necessary for the analytical model. The results from the developed analytical model were found to correlate well with experimental results.

Nomenclature

A^a	=	equivalent cross-sectional area of the aluminum beam
A^c	=	equivalent cross-sectional area of the composite panel
E^a	=	Young's modulus of the aluminum beam
E^c	=	Young's modulus of the composite panel
F	=	load transferred by the fasteners
L^a	=	length of a unit of the aluminum beam
L^c	=	length of a unit of the composite panel
P	=	bypass force
T	=	present temperature
T^a	=	equivalent temperature of the aluminum beam
T^c	=	equivalent temperature of the composite panel
T^o	=	initial temperature
u	=	displacement in the x direction
α^a	=	coefficient of thermal expansion of the aluminum beam
α^c	=	coefficient of thermal expansion of the composite panel
Δu_M	=	change in length due to mechanical load
Δu_T	=	change in length due to temperature change
ε	=	original strain-gauge reading
ε_M	=	strain due to tensile/compressive stress
ε_T	=	strain due to thermal expansion/contraction
ε_{T0}	=	strain-gauge output due to change in temperature

I. Introduction

GLOBAL competitiveness has become vital for airplane makers in recent years. To achieve higher fuel efficiency, the use of lightweight, high-strength composite materials, such as carbon/epoxy, needs to be fully explored. Large composite structures have been increasingly used in the aviation industry. New applications of composite materials include primary structures such as aircraft fuselages. These large composite parts are sometimes attached, either by the fasteners or adhesive bonding, to metallic structures. Computer software and test data are well established for calculating the mechanical loads of aircraft structures during flight, takeoff, and landing. However, thermally induced loads resulting from a large coefficient of thermal expansion (CTE) mismatch between the metallic and composite structures, such as those between aluminum frames and composite fuselage skins, have not been thoroughly investigated. The example used is a composite aircraft fuselage for which the fuselage skin is made of solid carbon/epoxy composite and is fastened to aluminum beams at the aircraft assembly line, which has a temperature of around 75°F. After the aircraft takes off and cruises at 35,000 ft above sea level, the ambient temperature can be as low as −65°F. Aluminum has a much larger CTE than composites; therefore, aluminum beams would shrink much more than composite skins, due to the 140°F temperature change if aluminum beams are separated from composite skin. However, the restraint from the composite skin, via fasteners, prohibits aluminum beams from contracting as much as they would. The interaction between the aluminum beams and the composite skin, via fasteners, generates tensile loads on the aluminum beams and, at the same time, compressive loads on the composite skin. The additional tensile loads on aluminum beams to flight loads would worsen their damage tolerance and fatigue capability, and so it is important to take into account the thermally induced loads when designing such structures.

There has been much work done in the area of thermal structures. Thornton [1] presented a review on research work in the thermal structures area conducted from the 1950s to the 1980s. All aspects of thermal structures of space vehicles, including aerodynamic heating, aerothermal load effects on flight structures, design of thermal structures, heat transfer, and thermal stresses were covered in his article. Specific studies found from the literature regarding issues due to CTE mismatch of composites focused mostly on the CTE mismatch between the fiber and matrix material. Mallick et al. [2] presented both analytical and experimental work toward reducing the thermal expansion of polymer-matrix materials for cryogenic composite tank applications. They proposed the addition of inclusions, nanoparticle reinforcements, which are much stiffer than the matrix to reduce the thermal expansion of the matrix. The effect of viscoelasticity of matrix material on the evolution of processing-induced residual stresses in glass-fiber/epoxy cross-ply laminate was investigated by Chen et al. [3] using a finite element micro-mechanical model. They found that although the CTE for the individual constituents (glass fiber and epoxy matrix) are constant,

Received 24 April 2007; accepted for publication 30 October 2007.

*Associate Professor, Airbus Fellow, Department of Aerospace Engineering.
†Research Associate, Department of Aerospace Engineering.
‡Manager/Senior Research Engineer, National Institute for Aviation Research.
§Graduate Research Assistant, Department of Aerospace Engineering.

the CTE for composite, on the other hand, is initially time-dependent due to the mismatch constraint and approaches an asymptotic value after a long stress-relaxation period. Analytical modeling of relaxation of strain due to CTE mismatch at the metal–ceramic interface of metal-matrix composites was developed by Taya et al. [4] using variational principle and Eshelby's method. Complete relaxation can be found by minimizing the total potential energy. As an example, a complete relaxation of a creeping metal-matrix composite is that the von Mises stress in the metal matrix becomes zero (i.e., hydrostatic state of stress).

Another area in which effects due to mismatch in CTE were studied is bonded repairs. The damaged aluminum panels are bonded with carbon/epoxy patches. One of the disadvantages of this method has been the introduction of thermal residual stresses in the repair due to the mismatch in CTE between the aluminum skin material and the repair material. Experimental as well as analytical work has been performed by Daverschot et al. [5] and Vlot et al. [6]. The effects of residual thermal stresses on fatigue crack growth of composite-bonded repair on aluminum plates were investigated experimentally by Zhong et al. [7]. They also developed a modified analytical model based on Rose's analytical solution and the Paris power law.

Although the physics due to CTE mismatch between dissimilar materials is the same, each different configuration (namely, bonded and fastened structures) is worth a thorough investigation.

The objectives of the current study were twofold: 1) to experimentally investigate the thermally induced stresses in fastened hybrids of aluminum and composite structure and 2) to develop an analytical model to simulate the physical system and predict the thermally induced loads.

Experiments were designed to test fastened aluminum/composite assemblies with the composite side exposed to a temperature changing from 75 to −65°F, which simulates the change in ambient temperature from the aircraft assembly line to the actual flight. Temperatures and strains were recorded in representative locations throughout the test article during testing. Effects due to the length of the aluminum beams on the thermally induced stresses were also included in the study.

An analytical model was developed to determine the load transfer among the composite panel, aluminum beams, and titanium fasteners. Parameters needed for the analytical model (namely, the equivalent cross-sectional areas of the composite panel and aluminum beams, the equivalent temperatures of the composite panel and aluminum beams, and the fastener stiffness) were determined by the reduced finite element models. Material properties (such as CTE, thermal conductivity, and tensile modulus, of the aluminum beam and composite panel) were either determined experimentally or obtained from the literature.

Although finite element analysis methods are capable of modeling the fastened composite/aluminum hybrid assembly and obtaining stress distributions and fastener loads, it takes a stress engineer a significant amount of time to build the full-scale finite element model of a large assembly to obtain accurate results. It would also take a significant amount of computation time when nonlinear contact elements are used in the fastener areas. With the developed analytical model, only reduced finite element models are needed to obtain the five required parameters for the analytical model. Parameters included in the analytical model (such as equivalent areas, Young moduli, and CTEs of the substrates and temperature change of the assembly) can be changed to analyze assemblies with different materials, shapes and geometries, and dimensions in other applications. In other words, the developed models can be applied not only to the aluminum/composite assemblies, but also to other fastened assemblies with dissimilar materials. Therefore, the model will assist designers in reducing structure loads caused by CTE mismatch. Full-scale experiments, as well as full-scale finite element analyses, can then be avoided to save both time and costs.

The test data and models obtained from this research will enable prediction and reduction of preload stress due to thermal issues in hybrids of aluminum and composite structures. This is an advanced technology category whereby aluminum composite hybrids are used in cases in which it would not be possible otherwise.

II. Experimental Approach

A. Test Article Configuration and Fabrication

As shown in Fig. 1, a test article 68 in. long and 36 in. wide with aluminum beams was used to simulate the solid composite laminate fuselage skin assembly. The width of 36 in. was chosen to accommodate three bays, each 12 in. wide, to isolate the central bay, which was used for all analyses, from the two side bays to avoid the influence of any edge effects of the assembly. The solid composite panel was fabricated with graphite/epoxy unitape and plain-weave fabric using a layup sequence of $[0_f/[45/0/-45/90]_4]_s$. The cured panel was trimmed at the four edges to obtain the final dimensions of $\frac{1}{4}$ by 36 by 68 in. Three 68-in.-long 7075-T6511 aluminum beams were fastened to the cured panel at the locations shown in Fig. 1 using $\frac{1}{4}$-in. titanium Hi-Locs®, each separated by 1 in. The cross section of the aluminum beam is shown in Fig. 2. A torque of 35 in. · lb was used to tighten the Hi-Locs.

For the purpose of studying the effects on length, six lengths were chosen based on finite element and analytical model simulations that show the trend of fastener-load transfer vs fastened length. Different lengths of the aluminum beams were achieved by fastening the aluminum beams to the composite panel with different numbers of fasteners, for which the maximum number of fasteners used was 66 and the available length of the composite panel was about 68 in. When 66 fasteners were used for each beam, the fastened length of the aluminum beams was 65 in. After tests were done with 66 fasteners, nine fasteners were taken out from each of the two ends (lengthwise) to shorten the fastened length to 47 in., with 48 fasteners on each beam. The six configurations are listed in Table 1. For each length configuration, different numbers of thermocouples and strain gauges were applied at different locations to record the temperature and strain data of the assembly. Strain gauges were attached to the top surface of the bottom flange (the 1.75-in.-wide flange shown in Fig. 2) of the aluminum beam at various locations along the length of

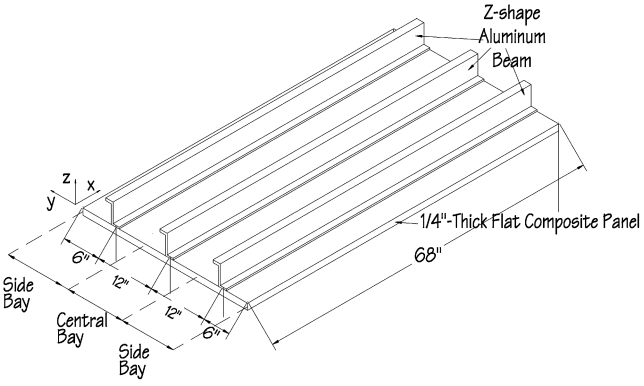

Fig. 1 Test article configuration.

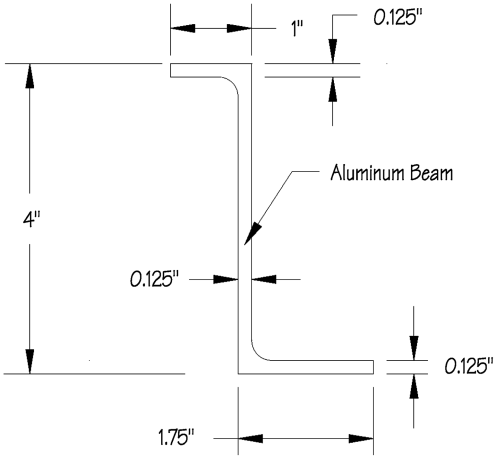

Fig. 2 Dimensions of cross section of Z-shaped aluminum beam.

Table 1 Test article length configurations

Length configuration	Fasteners used for each beam	Fastened length, in.
1	66	65
2	48	47
3	32	31
4	24	23
5	16	15
6	8	7

the beam. Figure 3 shows a typical setup using 66 fasteners on each beam. Each setup was tested at least twice to ensure repeatability.

B. Test Configuration

An environmental chamber, as shown in Fig. 4, was designed and fabricated to simulate the outside aircraft's temperature, which varies from the room temperature of 75°F to the actual flight temperature of −65°F. The chamber was designed to accommodate a test article 68 in. long and 36 in. wide. The outer wall of the chamber was made of plywood, and the inner walls were insulated by a 1.5-in.-thick rigid sheet of PVC foam. Liquid nitrogen was injected into the chamber at a controlled rate to cool down the air inside the chamber to a stable temperature of −65°F. Two fans were installed on the walls to generate air circulation. Z-shaped brackets were fastened on the top of the chamber walls, and the three-beam aluminum/composite assembly (test article) was placed on the Z-shaped brackets, as shown in Fig. 5. Weather stripping was used between the brackets and the composite panel to prevent cold-air leaks.

In the test configuration, the bottom surface of the composite panel was exposed to the −65°F cold air, and the Z-shaped aluminum beam was exposed to the room temperature of about 75°F. As shown in Fig. 6, the top surface of the composite panel between aluminum beams was insulated by a sheet of $\frac{3}{4}$-in.-thick polystyrene foam. This is to simulate the aircraft fuselage configuration in which an

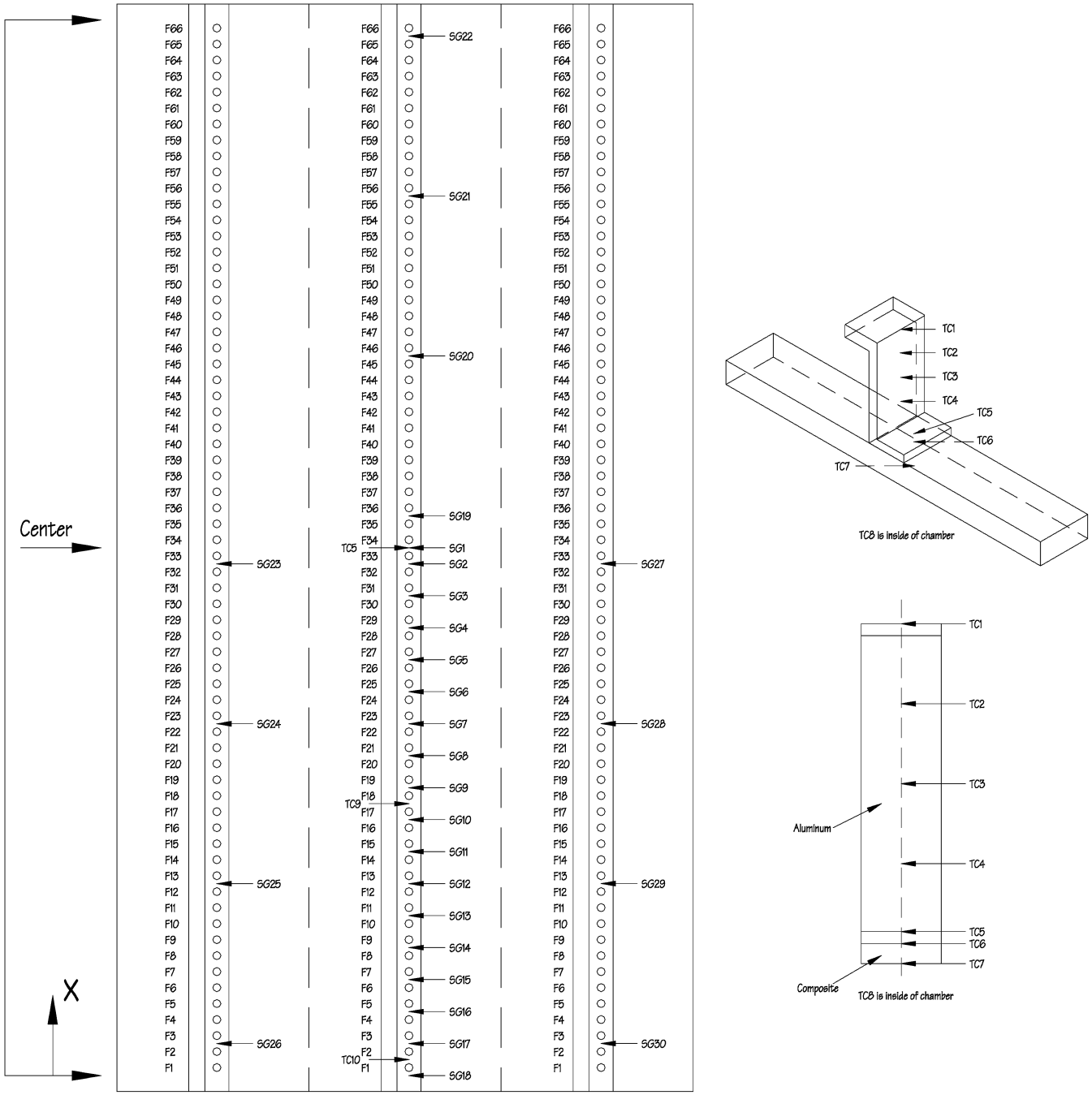

Fig. 3 Thermocouple and strain-gauge locations for the 66-fastener configuration with 10 thermocouples and 30 strain gauges.

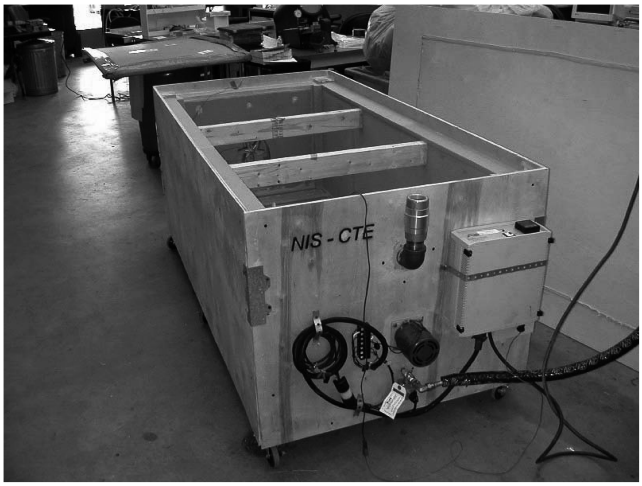

Fig. 4 Wooden environmental chamber.

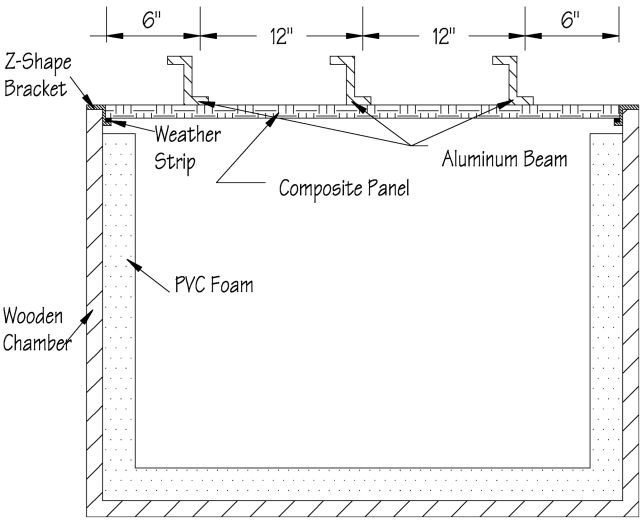

Fig. 5 Configuration of environment chamber with test article (side view).

insulation layer is added between the inner side of the fuselage and the cabin interior panels.

C. Test and Data Analysis Procedures

Liquid nitrogen was used to cool down the air inside the environmental chamber to −65°F with the control thermocouple located inside the chamber. Both temperature and strain data were monitored in real time by the StrainSmart data acquisition system (Vishay Measurements Group). The time history and steady state of temperature and strain were recorded.

Strain readings ε taken during the test included two components: 1) temperature output ε_{T0}, the output of the strain gauge due to the change in electric resistance of the gauge resulting from the change in temperature, and 2) the actual deformation of the strain gauge. The first component, temperature output ε_{T0}, was obtained by applying the polynomial supplied by the strain-gauge manufacturer (Vishay Micro-Measurements). A typical polynomial supplied by the gauge manufacturer is shown as

$$\varepsilon_{T0} = -2.79 \times 10^{2} + 5.99 \times 10^{0} T - 3.31 \times 10^{-2} T^{2} + 3.99 \times 10^{-5} T^{3} \quad (1)$$

where T represents the temperature at the instance when the strain data was recorded and Eq. (1) is valid from −100 to 350°F. The second component, the actual deformation, also included two parts: 1) thermal strain ε_T due to thermal expansion/contraction and

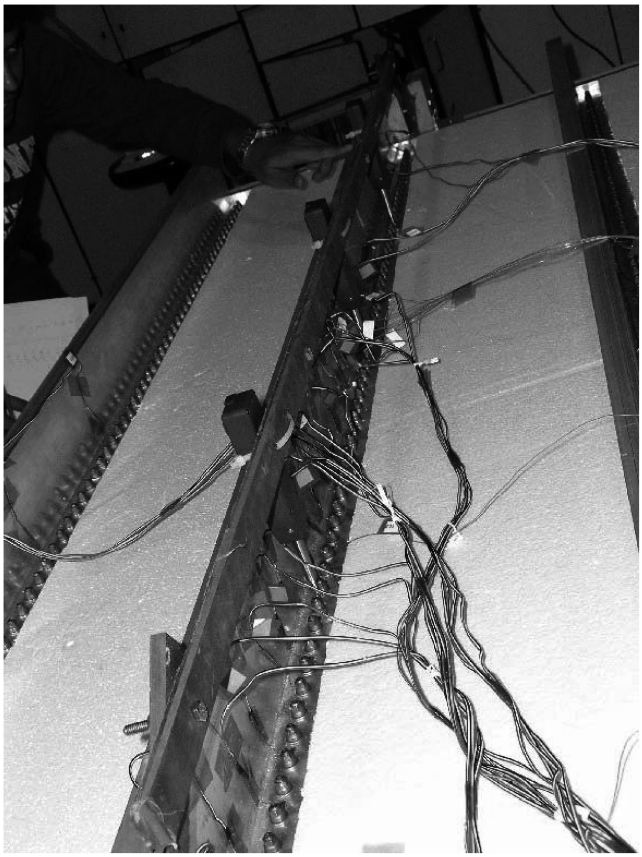

Fig. 6 Top surface of the composite panel covered by polystyrene foam (white color).

2) mechanical strain ε_M due to tensile/compressive stress. The thermal strain can be calculated by

$$\varepsilon_T = \alpha(T - T^o) \quad (2)$$

where α is the CTE of the aluminum beam, and T^o represents the initial temperature (75°F). Therefore, the mechanical strain, which can be converted to stress directly by multiplying Young's modulus, was obtained by adjusting the original strain reading ε by the thermal output ε_{T0} and the thermal strain ε_T:

$$\varepsilon_M = \varepsilon - \varepsilon_{T0} - \varepsilon_T \quad (3)$$

III. Analytical Approach

A. Analytical Model Development

As described earlier, the test article (as shown in Fig. 1) includes three bays, and only the strain data collected at the central bay was used for all analyses, to avoid any edge effects. The analytical model developed considers one bay of the assembly, which includes one aluminum beam and the 12-in.-wide composite panel to which the aluminum beam was fastened at its center, as shown in Fig. 7. For the convenience of analytical model development, the assembly was defined as a combination of identically fastened aluminum/composite units. Each unit was 1 in. in length in the x direction, and the length of each unit of the aluminum beam and composite panel were denoted as L^a and L^c, respectively, which were both 1 in. for the current configuration based on the fastener pitch. The free-body diagrams of each unit are shown in Figs. 8 and 9, which correspond to the aluminum beam and the composite panel, respectively. Because of the symmetry in the length direction (x direction), only half of the assembly was modeled. Figures 8 and 9 show only the left half of the entire assembly, and the centerline is located at the right end. According to the dial-gauge readings, which were taken in the out-of-plane direction (the z direction) of the middle beam during testing,

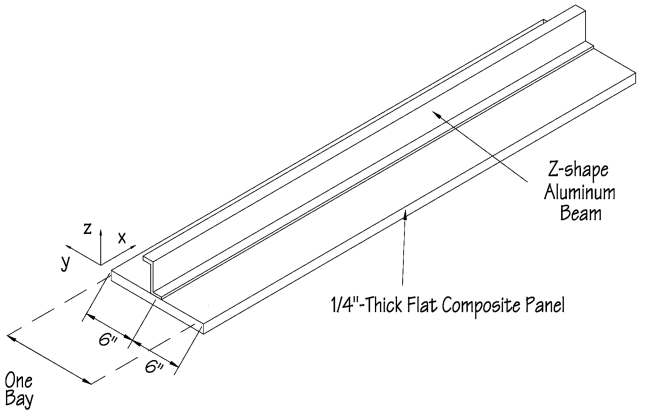

Fig. 7 One bay of aluminum/composite assembly test article.

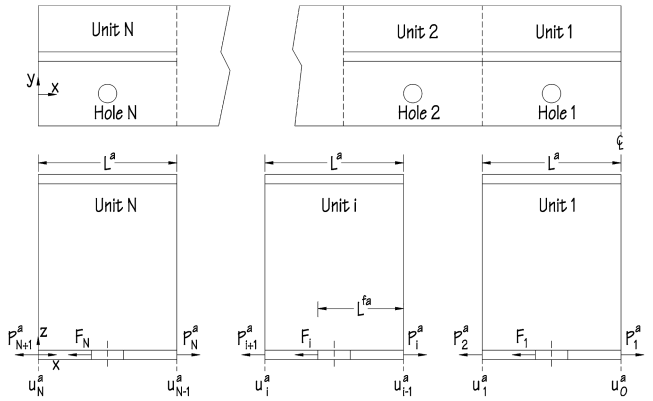

Fig. 8 Free-body diagram of Z-shaped aluminum beam.

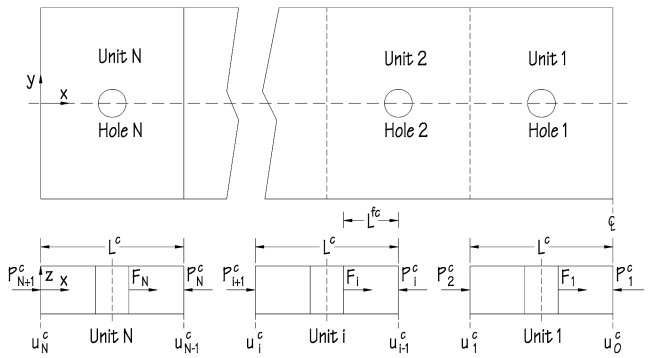

Fig. 9 Free-body diagram of flat composite panel.

the out-of-plane displacement is so small that the bending moment in the y direction can be neglected. Therefore, only the in-plane load transfer was considered in the free-body diagram and the model derivation. In the free-body diagrams, u_i and u_{i-1} denote the displacements of the two ends of the ith unit, where u is positive in the positive x direction, P_i represents the bypass force, F_i denotes the load transfer by the ith fastener, and the length of each unit is 1 in. Superscripts a and c denote the aluminum beam and composite panel, respectively. The center cross section, which is located at the right edge in Figs. 8 and 9, is fixed in the x direction because of symmetry, and the left edge, located at $x = 0$, is free to contract or expand.

The different temperature changes and different coefficients of thermal expansion between the aluminum beam and the composites panel would result in a different expansion/contraction. The fuselage skin, the outside surface of the composite panel, was exposed to a −65°F ambient temperature, and the aluminum beam was exposed to the 75°F room temperature, representing the interior of the aircraft cabin. Although the aluminum beam experiences smaller temperature changes compared with the composite panel, the aluminum beam contracts more than the composite panel, because the CTE of aluminum is much larger than the CTE of the composite panel if both contract independently. When the aluminum beam is fastened to the composite panel, the mismatch in contraction results in force interaction between the aluminum beam and the composite panel via the fasteners. The fasteners provide tensile forces on the aluminum beam to reduce its contraction and, at the same time, provide compressive forces on the composite panel to further reduce its length. Based on the free-body diagrams in Figs. 8 and 9, the force equilibrium conditions of the aluminum beam units and composite panel units in the x direction give

$$P_i^a - F_i - P_{i+1}^a = 0 \tag{4}$$

$$-P_i^c + F_i + P_{i+1}^c = 0 \tag{5}$$

where P is the bypass force, F is the load transferred by the fastener, $i = 1, \ldots, N$ specifies the unit number, and the superscripts a and c denote the aluminum beam and composite panel, respectively. The force boundary conditions at the edge of the panel are

$$P_{N+1}^a = 0 \tag{6}$$

$$P_{N+1}^c = 0 \tag{7}$$

Assuming that the displacement is uniform at each cross section perpendicular to the x direction, then the change in length of the ith unit of the aluminum beam due to temperature change, Δu_{iT}^a, from T^o to T^a is

$$\Delta u_{iT}^a = \alpha^a (T^a - T^o) L^a \tag{8}$$

where α^a is the CTE of aluminum, T^o represents the initial temperature or the temperature at which the aluminum beam/composite panel was assembled, and T^a represents the equivalent temperature of the aluminum beam at which the thermally induced stresses are to be determined. The equivalent aluminum beam temperature was used because the temperature distribution in the beam is not uniform: the upper flange of the Z-shaped aluminum beam has a higher temperature than the bottom flange, which is fastened to and has direct contact with the composite panel. The equivalent temperature T^a is to be determined by finite element analysis. Because of the load transferred by fastener F_i and the bypass load, the change in length of the ith unit of the aluminum beam due to mechanical load Δu_{iM}^a is

$$\Delta u_{iM}^a = \frac{F_i L^{fa}}{E^a A^a} + \frac{P_{i+1}^a L^a}{E^a A^a} \tag{9}$$

where L^{fa}, which is 0.625 in., represents the distance from the left edge of the fastener hole to the right edge of the unit, E^a is Young's modulus of aluminum, and A^a represents the equivalent cross-sectional area of the aluminum beam unit, which is to be determined by finite element analysis and remains constant for each unit. The change in length of the ith unit of the aluminum beam is

$$\Delta u_i^a = u_{i-1}^a - u_i^a = \Delta u_{iT}^a + \Delta u_{iM}^a \tag{10}$$

where u is positive in the positive x direction, and positive Δu means elongation. By substituting Eqs. (8) and (9) into Eq. (10), the kinematics equation of the ith unit of the aluminum beam becomes

$$u_{i-1}^a - u_i^a = \alpha^a (T^a - T^o) L^a + \frac{F_i L^{\mathrm{fa}}}{E^a A^a} + \frac{P_{i+1}^a L^a}{E^a A^a} \tag{11}$$

where $i = 1, \ldots, N$. The displacement boundary condition is

$$u_0^a = 0 \tag{12}$$

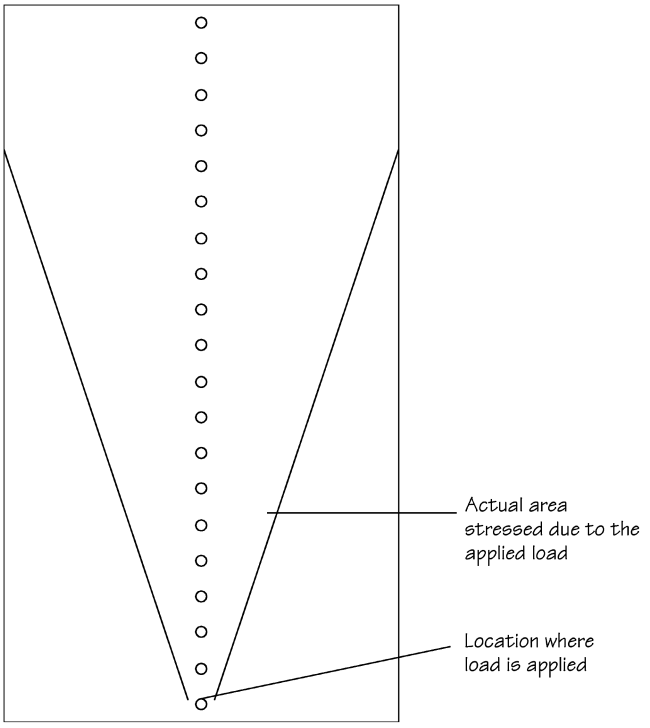

Fig. 10 Area influenced by external load in the wide composite panel.

Similarly, the change in length of the ith unit of the composite panel due to temperature change Δu^c_{iT} is

$$\Delta u^c_{iT} = \alpha^c (T^c - T^o) L^c \tag{13}$$

where α^c is the CTE of the composite panel, T^o represents the initial temperature or the temperature at which the aluminum beam/composite panel is assembled, and T^c represents the equivalent temperature of the composite panel at which the thermally induced stresses are determined. The length of the ith unit of the composite panel L^c is also 1 in.

The load transferred by the ith fastener F_i and the bypass force P^c_{i+1} compress the ith unit of the composite panel. The load applied from the fasteners to the composite panel is a concentrated load around the fastener hole. As shown in Fig. 10, the affected area, or the equivalent area of the composite panel that is used to calculate the elongation due to the fastener load, depends on the distance from which the load is applied. The equivalent area spreads up when it is farther from the location at which the load is applied, and the equivalent area will become the entire cross-sectional area of the composite panel within one bay, 12 by ÷ in., when it is a certain distance away from the load. The equivalent area of the composite panel, A^c_i, is also to be determined by finite element analysis, where the subscript i means that the area A^c_i is i units away from the loading point. Therefore, the change in length of the ith unit of the composite panel due to mechanical loads, Δu^c_{iM}, is the summation of the deformations due to all the fastener forces from the ith unit to the very left edge of the assembly.

$$\Delta u^c_{iM} = -\frac{F_i L^{fc}}{E^c A^c_{0.375}} - \sum_{j=i+1}^{N} \frac{F_j L^c}{E^c A^c_{j-i}} \tag{14}$$

where L^{fc}, which is 0.375 in., represents the distance from the right edge of the fastener hole to the right edge of the unit, and E^c is Young's modulus of the composite panel. Similar to the equivalent area, the equivalent temperature T^c also varies for each unit, and the values of T^c are obtained from finite element analysis. The change in length of the ith unit of the composite panel is

$$\Delta u^c_i = u^c_{i-1} - u^c_i = \Delta u^c_{iT} + \Delta u^c_{iM} \tag{15}$$

By substituting Eqs. (13) and (14) into Eq. (15), the kinematics equation of the ith unit of the composite panel becomes

$$u^c_{i-1} - u^c_i = \alpha^c (T^c - T^o) L^c - \frac{F_i L^{fc}}{E^c A^c_{@0.375}} - \sum_{j=i+1}^{N} \frac{F_j L^c}{E^c A^c_{@j-i}} \tag{16}$$

where $i = 1, \ldots, N$, and the displacement boundary condition is

$$u^c_0 = 0 \tag{17}$$

The governing equation of the fastener is

$$F_i = K_f \left(u^a_i - u^c_i \right) \tag{18}$$

where K_f represents the equivalent fastener stiffness, which is determined from finite element models.

If half of the assembly is discretized into N units, as shown in Figs. 8 and 9, then there are $5N + 4$ unknowns, including $N + 1$ bypass forces P^a_i on the aluminum beam, $N + 1$ bypass forces P^c_i on the composite panel, N fastener loads F_i, $N + 1$ displacements u^a_i of the aluminum units, and $N + 1$ displacements u^c_i of the composite units. In terms of the $5N + 4$ unknowns and all parameters, $5N$ governing equations can be obtained from Eqs. (4), (5), (11), (16), and (18) for $i = 1, \ldots, N$. With four equations based on boundary conditions [Eqs. (6), (7), (12), and (17)], there is a total of $5N + 4$ equations. The computer software Maple 10 was used to solve all governing equations. The calculated mechanical strains on the surface of the bottom flange of the aluminum beam between fasteners were compared with test data to validate the analytical model. Once the strains are validated, the loads transferred by the fasteners can be predicted.

B. Finite Element Models to Determine Parameters

Before solving all the governing equations, however, five parameters must be determined using finite element analysis. A total of six finite element models were constructed and executed to determine the five parameters needed for an analytical model. These five parameters were equivalent temperatures T^a and T^c; equivalent areas A^a and A^c of the aluminum and composite units, respectively; and equivalent stiffness K_f of the fasteners. To validate the analytical model, the mechanical strains obtained from the physical tests were compared with the strains calculated using the analytical model. The strain readings from the physical tests were the strains at the top surface of the bottom flange of the Z-shaped aluminum beam, as shown in Fig. 11. However, the mechanical strains calculated by the analytical model were the strains at the midplane of the bottom flange or the average strain through the thickness of the bottom flange of the Z-shaped aluminum beam. Therefore, one additional finite element model was executed to determine the bending factor β, which correlates the mechanical strains at the top surface and at the midplane of the bottom flange of the Z-shaped aluminum beam to compare the analytical results with experimental results.

ABAQUS/Standard 6.5 was used to develop all mechanical models, thermal models, and mechanical/thermal coupled models. Nonlinear analyses using linear 3D hex elements were conducted. Contact and friction were included in the finite element models.

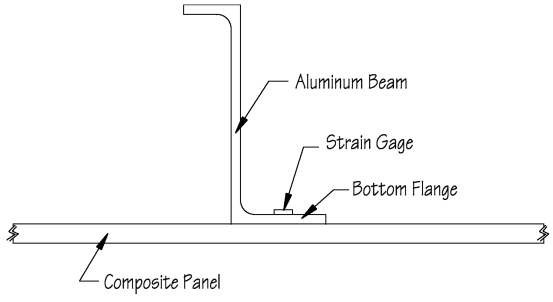

Fig. 11 Location of strain gauge.

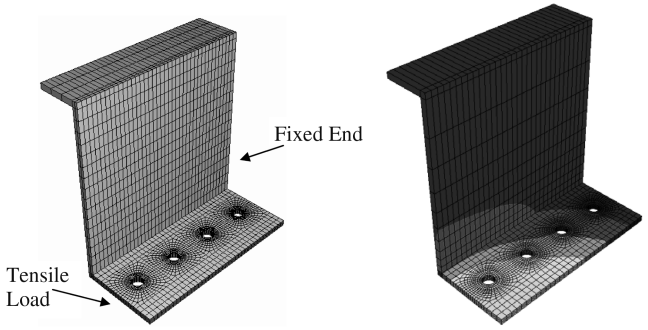

a) Boundary condition **b) Displacement contour**

Fig. 12 Mechanical finite element model of Z-shaped aluminum beam with four units.

1. Mechanical Finite Element Model to Determine A^a

To determine the equivalent area of the aluminum beam A^a, a mechanical finite element model of the Z-shaped aluminum beam with four units was constructed using ABAQUS 6.5, as shown in Fig. 12a. The right end of the model was fixed in the x direction, and a tensile load was applied at the left end.

As can be seen in the displacement contour shown in Fig. 12b, the displacement is not at all uniform at each cross section. This means that it is not reasonable to assume a uniform stress within each cross-sectional area and to use the entire cross-sectional area of the Z-shaped aluminum beam as A^a in the analytical model. Moreover, most of the deformation occurs at the bottom flange of the beam, which is where the loads are transferred from the fasteners. This is the reason that bypass loads and the fastener loads are presented at the bottom flange of the beam in the free-body diagram of Fig. 8. Therefore, the equivalent area A^a of the Z-shaped aluminum beam is obtained from the finite element model as

$$A_i^a = \frac{PL^a}{E^a \Delta u_i^a} \tag{19}$$

where P is the tensile load applied; L^a is the length of each unit of the aluminum beam (1 in.); E^a is Young's modulus of aluminum; and Δu_i^a, obtained from the results of finite element analysis, represents the elongation of the ith unit ($i = 1, \ldots, 4$). Even though the value of A^a for each of the four units is not exactly the same, they are within 0.62% of the average value. Therefore, a constant value of A^a was used for all units in the analytical model.

2. Mechanical Finite Element Model to Determine A^c

Similarly, a finite element model of the composite panel was constructed to determine the equivalent area A^c, as shown in Fig. 13. The 12-in.-wide composite panel was much wider than the aluminum beam, which had a width of 1.75 in. at the bottom flange. The displacement close to the location at which the load is applied is very nonuniform through the width, and the displacement becomes more uniform at locations further away from where the load is applied, as shown in Fig. 14. A finite element model with 20 units was needed to show this trend.

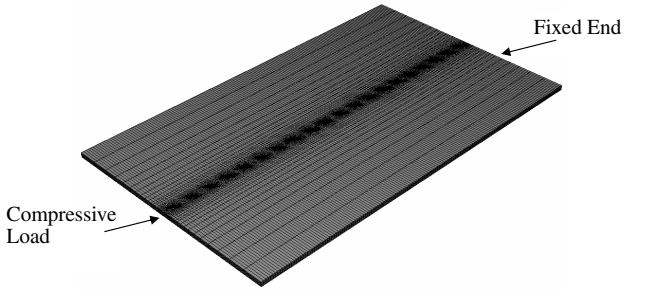

Fig. 13 Mechanical finite element model of flat composite panel with 20 units.

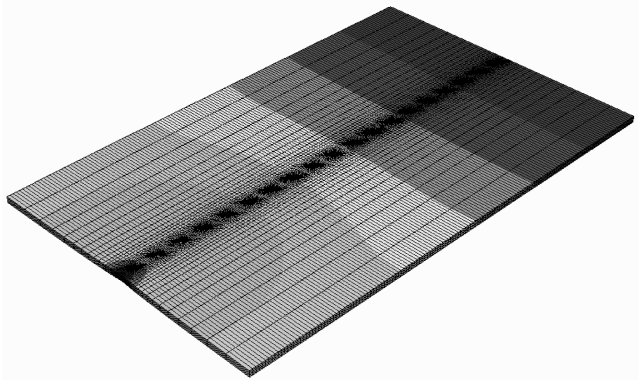

Fig. 14 Displacement contour of flat composite panel with 20 units.

Similar to the aluminum beam, the equivalent area of the composite unit can be obtained as

$$A_i^c = \frac{PL^c}{E^c \Delta u_i^c} \tag{20}$$

where P is the compressive load applied at the left end; L^c is the length of each unit of the composite panel (1 in.); E^c is Young's modulus of the composite panel; and Δu_i^c, obtained from the results of finite element analysis, represents the contraction of the ith unit ($i = 1, \ldots, 20$ and unit 1 is at the left end, where the compressive load is applied). As described previously, A^c is a function of the distance between the location at which the load is applied and the location at which A^c is calculated. Furthermore, A^c increases asymptotically to the entire cross-sectional area when the distance becomes large.

3. Thermal Finite Element Model to Determine Temperature Distribution

A heat transfer finite element analysis was conducted to achieve the proper temperature distribution in the steady-state heat transfer condition to determine temperature distribution within the aluminum beam/composite panel assembly during the environmental chamber test. The finite element model with four assembled units and boundary conditions is shown in Fig. 15. In this model, the aluminum beam was exposed to the 75°F room temperature, the bottom surface of the composite panel was exposed to −65°F cold air, and all other surfaces were insulated.

4. Coupled Thermal/Mechanical Finite Element Model to Determine T^a

It was verified by the thermal finite element model that the temperature distribution is nonuniform in the aluminum beam within each cross section: lower temperature at the lower flange and higher temperature at the upper flange. Because of the nonuniformity of the temperature distribution, it is not feasible to determine the equivalent

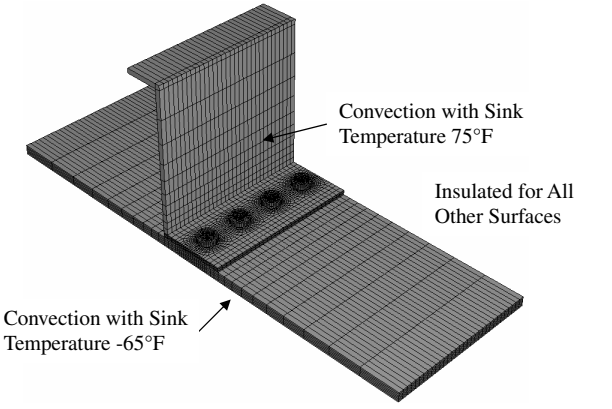

Fig. 15 Thermal finite element model of aluminum/composite assembly with four units.

temperature for the aluminum beam to be used in the analytical model directly from the temperature distribution. Therefore, a coupled thermal/mechanical finite element analysis was conducted on the Z-shaped aluminum beam with four units to determine the equivalent temperature T^a. In the finite element model, one of the two ends of the four-unit model is fixed, the rest of the beam was free to deform under the thermal load, and the temperature distribution obtained from the previous thermal finite element model was fed into the coupled thermal/mechanical model as the thermal load.

After the displacement field was obtained, the change in length of each aluminum unit Δu_i^a was recorded at the bottom flange, and the equivalent temperature of the ith aluminum beam unit T_i^a was back-calculated based on Eq. (8) as

$$T_i^a = T^o + \frac{\Delta u_i^a}{\alpha^a L^a} \tag{21}$$

where the initial room temperature T^o was 75°F, α^a was the CTE of aluminum, and the unit length of each aluminum beam unit L^a was 1 in.

5. Coupled Thermal/Mechanical Finite Element Model to Determine T^c

Using the same approach to determine T^a, the equivalent temperature T^c was determined using a coupled thermal/mechanical finite element model on the composite panel. The same concept used in determining the equivalent area of the composite panel, as described previously, was applied to determine the equivalent temperature, which is a function of location. The equivalent temperature, as a function of distance, was obtained by

$$T_i^c = T^o + \frac{\Delta u_i^c}{\alpha^c L^c} \tag{22}$$

where Δu_i^c is the change in length of the ith composite unit at the central location, α^c is the CTE of the composite, and the length of each unit of the composite panel, L^c, is 1 in.

6. Coupled Thermal/Mechanical Finite Element Model to Determine K_f

To determine the fastener stiffness K_f, a finite element model of the fastened aluminum/composite assembly with eight units, as shown in Fig. 16, was constructed using temperature as the thermal load, along with a fixed boundary condition at the right end. In the finite element model, *surface contact* was defined between the fastener and the aluminum hole, between the fastener and the composite hole, and between the aluminum/composite contact surfaces. The behavior between perpendicular surfaces in contact was established as *hard contact*, which means no penetration was allowed. The tangential surface behavior was governed by the penalty friction formulation. For most surfaces, the coefficient of friction μ is normally less than unity. The effective friction coefficient at the fastener/panel interface was set at $\mu = 0.07$, which was obtained through trial-and-error modeling by Pratt et al. [8]. A value of $\mu = 0.2$ was used for the panel/panel interface, based on the experimental results by Pratt et al.

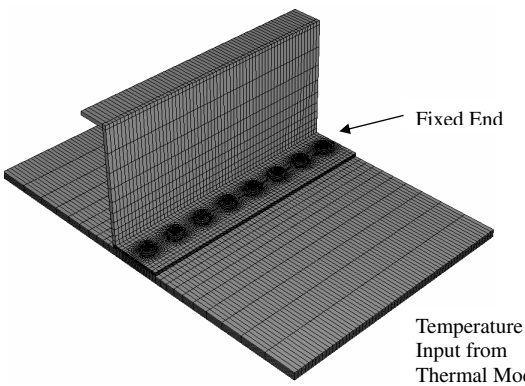

Fig. 16 Eight-unit fastened aluminum/composite assembly model.

In each unit, the load transferred by the ith fastener F_i is defined as the summation of contact force between the fastener and the hole and the friction between the aluminum and composite surfaces. Both the contact force and friction were obtained from finite element analysis. The displacements of each unit of the aluminum beam and the composite panel, u_i^a and u_i^c, respectively, were recorded. The equivalent fastener stiffness was calculated as

$$K_{\text{fi}} = \frac{F_i}{u_i^a - u_i^c} \tag{23}$$

From the preceding, five parameters (equivalent areas A^a and A^c, equivalent temperatures T^a and T^c, and equivalent fastener stiffness K_f) were obtained from finite element analyses. By substituting these parameters into the analytical model, the stress distribution and load transfer can be calculated.

As described previously, the bending factor β is necessary to convert the midplane strain of the bottom flange of the Z-shaped aluminum beam to the strain at the top surface of the flange to compare the physical test results with the analytical model. The same finite element model used to determine the fastener stiffness K_f was used for this purpose. The bending conversion factor is defined as β_i for the ith unit as

$$\beta_i = \frac{\varepsilon_i^{\text{top}}}{\varepsilon_i^{\text{center}}} = \frac{\varepsilon_i^{\text{top}} E^a A^a}{P_i} \tag{24}$$

where the strain at the top surface of the bottom flange $\varepsilon_i^{\text{top}}$ is extracted from the finite element model, and the bypass load P_i is obtained from the finite element model as well. Because only mechanical strains are considered, the Z-shaped aluminum beam is under tension loads from the fasteners at the bottom flange. The bottom flange bends up so that strain at the top surface is smaller than strain at the center. Therefore, the value of β is less than 1. Because the bending effect is small, the value of β is very close to 1. This also validates the assumption that only in-plane forces need to be considered.

IV. Results and Discussion

To study the effects of length, six different configurations with different fastened lengths were tested. They were a 66-fastener setup (fastened length was 65 in. with 1-in. pitch), a 48-fastener setup (fastened length was 47 in.), a 32-fastener setup (fastened length was 31 in.), a 24-fastener setup (fastened length was 23 in.), a 16-fastener setup (fastened length was 15 in.), and an 8-fastener setup (fastened length was 7 in.). The 66-fastener setup was tested first, and fasteners were taken out evenly from the two ends to reduce the fastened length to 47, 31, 23, 15, and 7 in. Each setup was tested at least twice to ensure repeatability.

A. Temperature Distribution

The temperature distributions in the steady state were similar for different fastened-length tests. Figure 17 shows the typical temperature history in the test, and the thermocouple locations are described in Fig. 3. With an inside chamber temperature of −65°F and outside room temperature of 75°F, there was a 55°F temperature difference between the bottom surface of the composite panel and the top surface of the aluminum bottom flange, as shown in Fig. 18.

B. Material Properties

Results from the material property tests are shown in Table 2, along with values found from the literature. The numbers obtained from the tests were used in the analytical model and finite element models.

C. Parameters from Finite Element Models

As described previously, six parameters (equivalent area for aluminum beam A^a and composite panel A^c, equivalent temperature for aluminum beam T^a and composite panel T^c, equivalent fastener

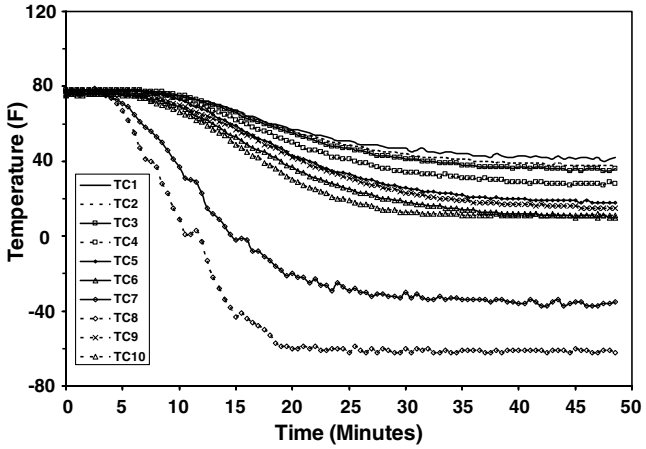

Fig. 17 Typical temperature history.

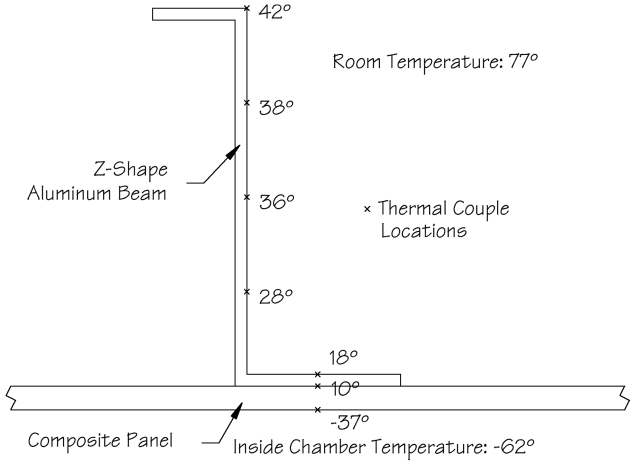

Fig. 18 Average temperature distribution of tests.

stiffness K_f, and bending factor β) were determined by finite element analyses. The temperature profile obtained from the heat transfer finite element model, which was used for the thermal/mechanical models, is shown in Fig. 19. Compared with Fig. 18, the temperature profile at the aluminum beam portion correlates the experimental results very well. The deviation of the temperature at the composite panel surface exposed to the cold air is due to the difficulty in obtaining accurate convection and contact heat transfer coefficients. The results on the five parameters are shown in Tables 3–5. The distance used in Table 4 is the relative distance between the point at which the equivalent area is calculated and at which the load is applied. The x coordinate used in Table 5 is the global x coordinate, as specified in Figs. 1–3. It can be seen that the equivalent area A^c increases when distance increases, until A^c reaches its asymptotic value.

The bending factor β calculated is 0.9, which means that the strain at the top surface of the aluminum bottom flange is very close to the strain at the midplane of the aluminum bottom flange. In another words, the bending effects in the assembly are very small.

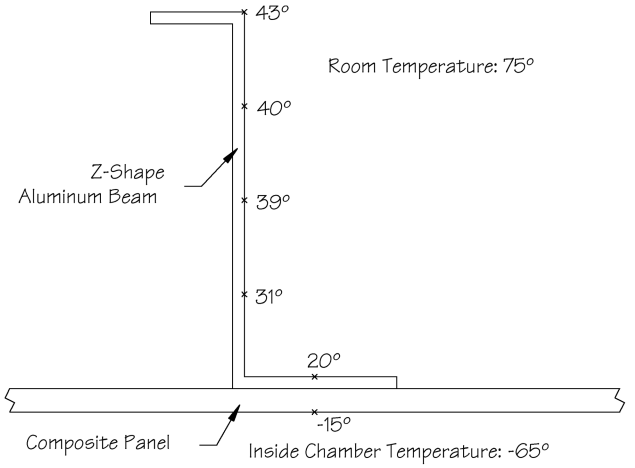

Fig. 19 Temperature profile determined from thermal finite element model.

D. Test Results and Comparison with Analytical Model

Mechanical strains at the top surface of the aluminum bottom flange were recorded for each setup. For all cases with different fastened lengths, the peak strain of the aluminum beam always occurred around the center of the fastened assembly, because the strain was accumulated from the free ends and reached the maximum value at the center. The peak strain increased when the fastened length increased and was tapered off after the fastened length reached a certain value.

After the six parameters for fastened aluminum/composite assembly were substituted into the analytical model, the mechanical strains were solved and compared with test results, as shown in Figs. 20–25, in which the mechanical strains were normalized by the overall maximum strain obtained from the tests. As can be seen from these figures, the analytical results correlate reasonably well with the test results. The strain-gauge reading at the center of the 66-fastener setup deviated from the analytical result. This was believed to be due to gauge malfunction, because the mechanical strain of the aluminum beam should be tapered off around the central portion of the length. An abrupt drop in strain value at the center is not reasonable. The peak strain varies with fastened length, as predicted by the analytical model, and the results correlate reasonably well with the test results, as shown in Fig. 26.

E. Load Transfer Prediction

Once the analytical model is validated, the load transfer of each fastener in the aluminum beam/composite panel assemblies can be predicted. The predicted fastener-load distributions by the analytical model for the assemblies of different fastened lengths are shown in Fig. 27. It is noted that the peak stress of the aluminum beam occurs at the center of the assembly, as described in the previous section. This is because stress accumulates from the free ends and finally peaks at the center. However, the load transfer through the fasteners shows the opposite trend. The end fasteners take the highest load, and the fasteners at the center carry very little load. The peak fastener load vs fastened length of the assembly is shown in Fig. 28. It can be seen that the maximum fastener load in the assembly reaches its asymptote at the fastened length of about 10 in. In other words, unless the

Table 2 Material properties

	Young's modulus, Msi		Poisson's ratio	Thermal conductivity at 73°F ($\times 10^{-6}$ Btu/in. · s · °F)		CTE ($\times 10^{-6}$/°F)	
Material	Literature [9]	Test	Test	Literature [9]	Test	Literature [9]	Test
Aluminum beam	10.5	10.878	0.328	1750	——	12.2	10.90
Composite panel	——	7.975	0.323	——	4.75	——	1.446
Titanium fastener	16.9	——	0.31	100	——	4.8	——

Table 3 Parameters for fastened aluminum/composite assembly

Material	Equivalent area A, in.^{2}	Equivalent temperature T, °F	Equivalent stiffness K, lb/in.
Aluminum beam	0.25	22	——
Composite panel	Varied (shown in Table 4)	Varied (shown in Table 5)	——
Titanium fastener	——	——	4.5×10^5

Table 4 Normalized equivalent area for composite panel

Distance, in.	0.375	1	2	3	4	5	6	7	8	9	10
A^c, in.^{2}	0.12	0.16	0.27	0.37	0.47	0.56	0.64	0.71	0.78	0.83	0.88
Distance, in.	11	12	13	14	15	16	17	18	19	20	
A^c,[a] in.^{2}	0.91	0.94	0.96	0.98	0.98	0.99	0.99	0.99	1.00	1.00	

[a]The equivalent area of the composite panel A^c remains constant when distance equals or exceeds 19 in.

Table 5 Normalized equivalent temperature for composite panel

x, in.	0	1	2	3	4	5	6	7
T^c,[a] °F	0.26	0.42	0.63	0.81	0.91	0.95	0.98	1.00

[a]The equivalent temperature of the composite panel T^c remains constant when x equals or exceeds 8 in.

assembly is shorter than 10 in., the largest fastener load is almost the same for the geometry and materials used in the current study.

V. Conclusions

A composite panel/aluminum beam assembly, 68 by 36 by 0.25 in., was fabricated and tested using a custom-designed/built environmental chamber. To simulate the actual flight situation, the bottom surface of the composite panel was exposed to −65°F cold air

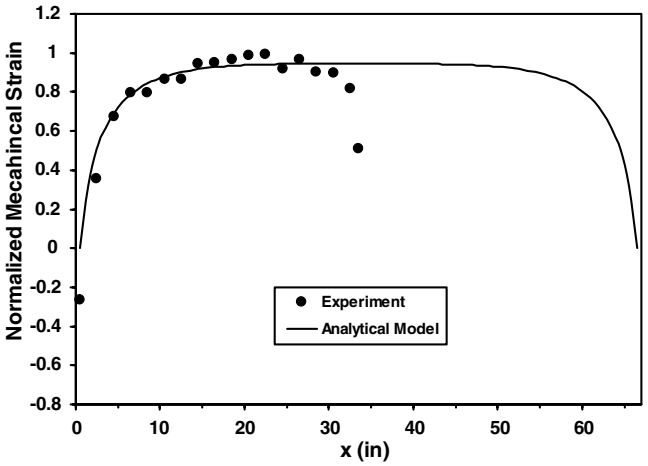

Fig. 20 Mechanical strains comparison between tests and analytical model for 66-fastener setup (65-in. fastened length).

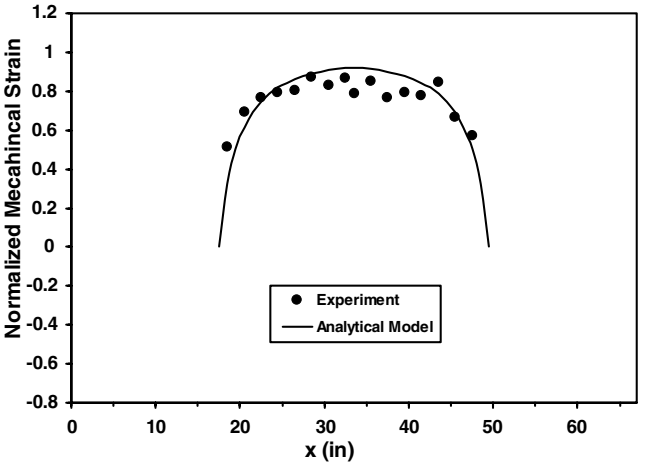

Fig. 22 Mechanical strains comparison between tests and analytical model for 32-fastener setup (31-in. fastened length).

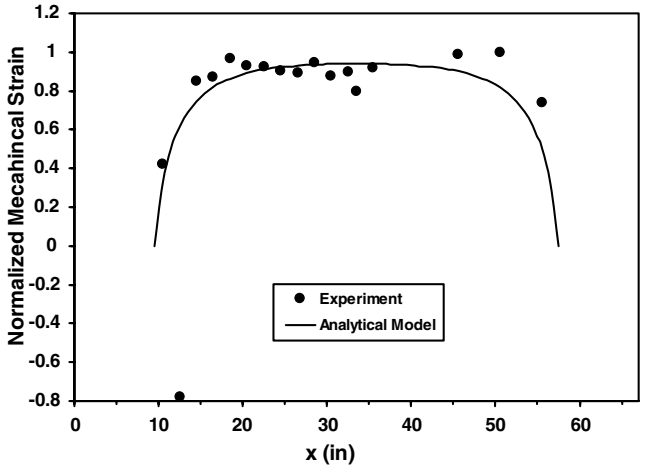

Fig. 21 Mechanical strains comparison between tests and analytical model for 48-fastener setup (47-in. fastened length).

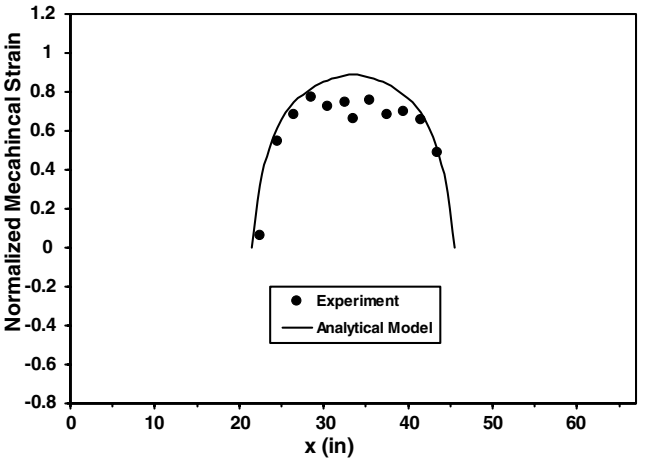

Fig. 23 Mechanical strains comparison between tests and analytical model for 24-fastener setup (23-in. fastened length).

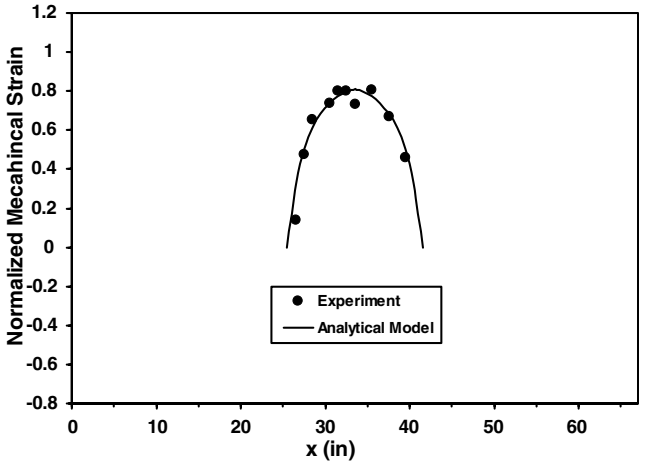

Fig. 24 Mechanical strains comparison between tests and analytical model for 16-fastener setup (15-in. fastened length).

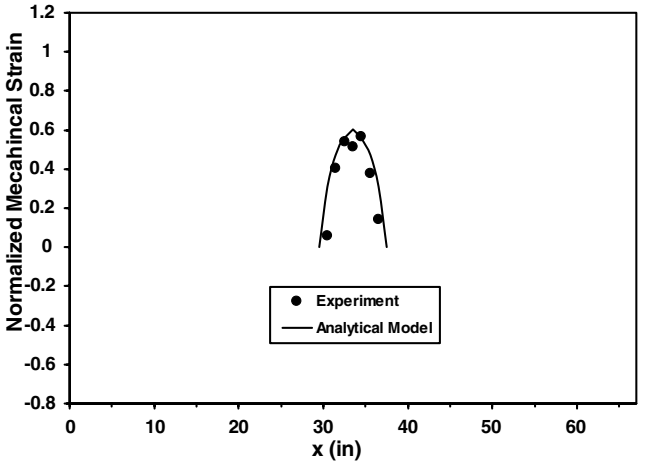

Fig. 25 Mechanical strains comparison between tests and analytical model for 8-fastener setup (7-in. fastened length).

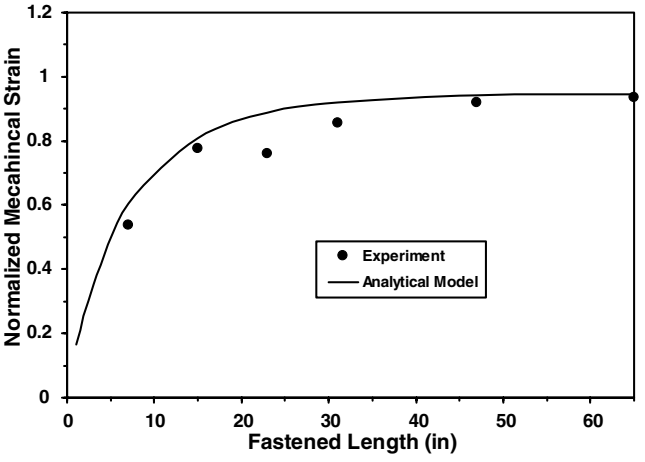

Fig. 26 Peak mechanical strains comparison between tests and analytical model for different fastened lengths.

inside the chamber, and the aluminum beams were exposed to 75°F room-temperature air. Temperature and strain distributions were recorded during the tests, and the steady-state temperature and strain distributions were analyzed.

In the assemblies, a 55°F temperature differential existed between the bottom surface of the composite panel and the top surface of the aluminum beam's bottom flange under the steady-state condition.

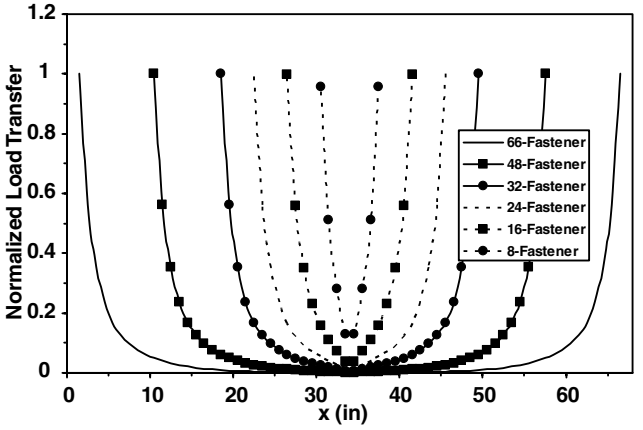

Fig. 27 Fastener-load transfer distribution for different fastened lengths.

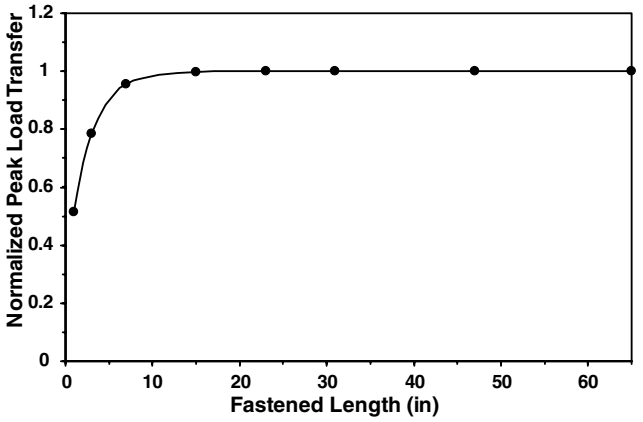

Fig. 28 Peak fastener-load transfer as a function of fastened length.

The maximum thermally induced stress of the aluminum beam occurred at the center in the length direction of the aluminum beam. The fasteners at the two ends of the assembly carried the maximum load transfer. The influence of the fastened length was also investigated. Six setups of different fastened lengths were tested for the assembly. It was found that the maximum stress of the aluminum beam due to CTE mismatch increases when the fastened length increases. However, the stress reached its asymptote after the fastened length equals or exceeds about 32 in.

An analytical model was developed to simulate the response of the fastened aluminum/composite assembly under thermal loads. Necessary parameters such as equivalent area, equivalent temperature, and equivalent fastener stiffness were determined by finite element analyses. The analytical model was validated by comparing the strain readings from the test article. Therefore, the response of the assembly to temperature change was captured by the model. With the developed analytical model, the fastener-load transfer of the assembly can also be predicted. The calculated fastener load shows the trend that the maximum fastener load reaches the asymptote when the fastened length equals or exceeds 10 in.

The developed methodology can be applied to similar fastened hybrids of metal and composites to determine thermally induced stress and fastener loads. Only reduced finite element models are necessary for the calculation of the five parameters needed for the analytical model. Full-scale experiments, as well as full-scale finite element models, can then be avoided to save both time and costs.

Acknowledgments

This study was supported by the state of Kansas under contract number NIS05-002. The investigators of this project would like to

thank the industrial points of contact of this project for their support and assistance: Jeff Swada and Gary Kreps from Spirit AeroSystems (formerly Boeing Wichita), Jim Krone from Cessna Aircraft Company, Melanie Violette and Randy Parker from Hawker Beechcraft (formerly Raytheon Aircraft Company), and Mike Klemanovic from Bombardier Learjet.

References

[1] Thornton, E. A., "Thermal Structures: Four Decades of Progress," *31st AIAA/ASME/ASCE/AHS/ASC Structures, Structural Dynamics, and Materials Conference*, AIAA, Washington, DC, 2–4 Apr. 1990, pp. 794–814.

[2] Mallick, K., Cronin, J., and Arzberger, S., "Effect of Inclusion Morphology on the Coefficient of Thermal Expansion of a Filled Polymer Matrix," *47th AIAA/ASME/ASCE/AHS/ASC Structures, Structural Dynamics, and Materials Conference*, AIAA, Reston, VA, 1–4 May 2006, pp. 1–10.

[3] Chen, Y., Xia, Z., and Ellyin, F., "Evolution of Residual Stresses Induced During Curing Processing Using a Viscoelastic Micro-mechanical Model," *Journal of Composite Materials*, Vol. 35, No. 6, 2001, pp. 522–542.
doi:10.1177/002199801772662145

[4] Taya, M., Lee, J. K., Dunn, M., Walker, G., and Mori, T., "High Temperature Behavior of Metal Matrix Composites," U.S. Air Force Office of Scientific Research, Rept. AFOSR-TR-96-0388, 1996.

[5] Daverschot, D. R., Vlot, A., and Woerden, H. J. M., "Thermal Residual Stresses in Bonded Repairs," *Applied Composite Materials*, Vol. 9, No. 3, 2002, pp. 179–197.
doi:10.1023/A:1014790304207

[6] Vlot, A., Verhoeven, S., Ipenburg, G., Siwpersad, D. R. C., and Woerden, H. J. M., "Stress Concentrations Around Bonded Repairs," *Fatigue and Fracture of Engineering Materials and Structures*, Vol. 23, No. 3, Mar. 2000, pp. 263–276.
doi:10.1046/j.1460-2695.2000.00245.x

[7] Zhong, W. H., Zhamu, A., Aglan, H., Stone, J., and Gan, Y. X., "Effect of Residual Stresses on Fatigue Crack Growth Behavior of Aluminum Substrate Repaired with a Bonded Composite Patch," *Journal of Adhesion Science and Technology*, Vol. 19, No. 12, 2005, pp. 1113–1128.
doi:10.1163/156856105774382426

[8] Pratt, J. D., and Pardeon, G., "Numerical Modeling of Bolted Lap Joint Behavior," *Journal of Aerospace Engineering*, Vol. 15, No. 1, 2002, pp. 20–31.
doi:10.1061/(ASCE)0893-1321(2002)15:1(20)

[9] "Metallic Materials Properties Development and Standardization (MMPDS)," U.S. Department of Transportation, Rept. DOT/FAA/AR-MMPDS-01, National Technical Information Service, Springfield, VA, 9 Dec. 2004.